Two-dimensional ^{1}H and ^{1}H-detected NMR study of a heterogeneous biocatalyst using fast MAS at high magnetic fields

Sabu Varghese,*[a] Peter J. Halling,[b] Daniel Häussinger[c] and Stephen Wimperis*[a]

[a]*Department of Chemistry, Lancaster University, Lancaster LA1 4YB, UK*

[b]*WestCHEM, Department of Pure & Applied Chemistry, University of Strathclyde, Glasgow G1 1XL, UK*

[c]*Department of Chemistry, University of Basel, CH-4056 Basel, Switzerland*

Keywords:

immobilized enzymes; heterogeneous biocatalysts; solid-state NMR, biocatalysis; ^{1}H MAS NMR; epoxy-functionalized silica; human carbonic anhydrase II; hCA II; covalent immobilization

Abstract

Nuclear magnetic resonance (NMR) is a powerful tool for investigating atomic-scale structure in heterogeneous or composite materials where long-range order is absent. In this work solid-state ^{1}H and ^{1}H-detected NMR experiments were performed with fast magic angle spinning (ν_R = 75 kHz) and at high magnetic fields (B_0 = 20 T) and used to gain structural insight into a heterogeneous biocatalyst consisting of an enzyme, human carbonic anhydrase II (hCA II), covalently immobilized on epoxy-functionalized silica. Two-dimensional ^{1}H-^{1}H NOESY-type correlation experiments were able to provide information on ^{1}H environments in silica, epoxy-silica and the immobilized enzyme. Two distinct signals originating from water protons were observed: water associated with the surface of the silica and the water associated with the immobilized enzyme. Additional two-dimensional ^{1}H-^{1}H double–single quantum (DQ-SQ) correlation experiments suggested that the immobilized enzyme is not in close contact with the silica surface. Most significantly, comparison of two-dimensional ^{1}H-^{15}N spectra of the immobilized enzyme and the solution-state enzyme confirmed that the structural integrity of the protein is well preserved upon covalent immobilization.

Introduction

Protein immobilization on solid supports and surfaces plays a crucial role in a range of technological applications including industrial biocatalysis, drug delivery, medical diagnosis, and biosensing.[1-2] Heterogeneous biocatalysis involves the conversion of chemical or biological substances using immobilized enzymes or cells[3-4] and is employed in industrial applications for the large scale synthesis of a wide variety of fine chemicals.[5] Little is known about the atomic-level structure of heterogeneous biocatalysts as conventional structural characterization methods, such as X-ray crystallography and solution-state NMR, cannot be directly employed. However, magic angle spinning NMR (MAS NMR) can be used to characterize heterogeneous systems and has been demonstrated in the study of a variety of immobilized enzymes and supports.[6-15] In a similar context, it should be noted that MAS NMR has also very been successfully employed in understanding the molecular level interactions of peptides and proteins with non-biological surfaces involved in biomineralization.[16-26]

Among the various means of immobilizing enzymes on solid supports, covalent immobilization has proven to be the most stable as leaching of the enzyme from the support is minimized. However, the state of the enzyme and changes in its dynamics upon immobilization are not well understood. Recently, we have been able to show that the structural integrity of an enzyme was not drastically changed upon immobilization and was comparable to that in the lyophilized state by using a model enzyme human carbonic anhydrase II (hCA II) covalently immobilized on epoxy-silica.[27] Since the lyophilized state of a protein may not necessarily be identical to the native structure in solution, better insight into the native fold of the protein before and after immobilization can be obtained by comparing, for example, the two-dimensional

solution-state ^{1}H-^{15}N HSQC NMR spectrum with that of the immobilized enzyme. In this research work, solid-state ^{1}H and ^{1}H-detected NMR experiments utilizing fast MAS (ν_R = 75 kHz) at high magnetic fields (B_0 = 20 T)[28] have been employed to characterize a model enzyme (hCA II) covalently immobilized on epoxy-silica. Protein samples were prepared in both isotopic natural abundance and in isotopically enriched (^{15}N) states (uniformly labelled samples termed hereafter as [U-^{15}N]/hCA II). Furthermore, to reduce spectral overcrowding in multidimensional MAS NMR experiments, hCA II samples were selectively ^{15}N labelled for the most abundant amino acid residue leucine (samples termed hereafter as [^{15}N Leu]/hCA II). Our results show that two-dimensional ^{1}H MAS NMR methods can be successfully employed with fast MAS to characterize the different proton environments in the silica support, covalent linker, and the immobilized enzyme. Comparison of two-dimensional ^{1}H-^{15}N spectrum from the immobilized enzyme and the solution-state NMR spectrum confirms that the structural integrity of the protein is well preserved upon covalent immobilization.

Experimental

Materials and sample preparation

The hCA II plasmid (pACA) used for the production of hCA II mutants was a generous gift from Carol A. Fierke (University of Michigan, USA).[29] Expression, purification, and characterization of [U-^{15}N]/hCA II and [^{15}N Leu]/hCA II were performed as described previously.[27, 30] Synthesis of epoxy-silica using SP-100-15-P Daiso silica gel and (3-glycidyloxypropyl)trimethoxysilane (GLYMO) as the covalent linker, immobilization of [U-^{15}N]/hCA II and [^{15}N Leu]/hCA II on epoxy-silica, and the biochemical characterization were performed as described previously.[27]

Solution and solid-state NMR experiments

Solution-state NMR experiments were carried out on a Bruker Avance III HD spectrometer operating at 600 MHz ^{1}H frequency, equipped with a cryogenic QCI probe ^{1}H/^{13}C/^{15}N/^{19}F with z-axis pulsed field gradients. Solid-state NMR experiments were performed on a Bruker Avance III 850 MHz spectrometer with a widebore 20 T magnet (850 MHz ^{1}H frequency). The dry powdered samples were packed into 1.0 mm ZrO_2 rotors and were spun at a frequency of 75 kHz. Chemical shifts were referenced externally relative for ^{1}H (adamantane: 1.87 ppm) and ^{15}N (glycine: 32.4 ppm). Two-dimensional ^{1}H-^{1}H correlation experiments were performed either with a NOESY-type (Nuclear Overhauser Effect SpectroscopY) sequence consisting of three simple 90° pulses[31] or with a double–single quantum (DQ-SQ) sequence utilizing BABA (BAck-to-BAck)[32] recoupling. For two-dimensional ^{1}H-^{15}N correlation, pulse sequences utilized linearly ramped cross-polarization (CP)[33-35] and small phase incremental alternation (SPINAL)[36] ^{1}H decoupling. All experiments were performed at room temperature. All NMR data were processed using TopSpin software. Further experimental and processing details can be found in the text and figure captions.

Results and discussion

To gain greater insight into the ^{1}H environments present during the different stages of enzyme immobilization, we performed two-dimensional ^{1}H-^{1}H correlation experiments on silica, epoxy-silica and immobilized hCA II using NOESY-type pulse sequences. Fig. 1 shows two-dimensional ^{1}H-^{1}H NOESY spectra of (a) silica, (b) epoxy-silica, (c) [U-^{15}N]/hCA II immobilized on epoxy-silica and (d) [^{15}N Leu]/hCA II immobilized on epoxy-silica recorded using a mixing time of 100 ms on a B_0 = 20 T magnet at a MAS frequency of ν_R = 75 kHz. The spectra are well resolved and reveal

diagonal peaks and off-diagonal or cross peaks; the latter may arise from either chemical exchange or from spin diffusion, both incoherent processes, during the mixing time. Cross peaks ascribed to the spin diffusion mechanism and with high intensity may cautiously be interpreted as arising from two nuclei that possess a strong mutual dipolar coupling and hence are close in space. Indeed, the 100 ms mixing time duration was selected as a compromise between cross-peak intensity and the desire to facilitate this interpretation. It has been reported that the use of radiofrequency-driven recoupling (RFDR) during the NOESY mixing time can increase the rate of ^{1}H-^{1}H polarization transfer.[37]

The NOESY spectrum of bare silica (Fig. 1a) features diagonal peaks appearing from isolated silanol groups (iOH, 1.1 ppm), physisorbed water (H_2O, 4.0 ppm) and hydrogen-bonded silanol groups (hBS, 4.5 to 9.0 ppm). The chemical shift assignments use the labelling scheme shown in Fig. 2, where the simplified representation of the hydrogen bonding of water with surface silanol groups is based on previous reports.[38] The peak from physisorbed water (4.0 ppm) is relatively narrow when compared with the broad peak from the hBS (4.5 to 9.0 ppm) indicating the presence of dynamics to average out anisotropic spin interactions. The hBS peak broadening (4.5 to 9.0 ppm) can be ascribed to the absence of dynamics and the inhomogeneous broadening associated with a wide range of chemical shifts contributed by the different modes of hydrogen bonding between surface silanol groups.[39] Intense cross peaks can be observed (4.0 ppm – 4.5 to 9.0 ppm) between physisorbed water and hBS (4.0 ppm – 4.5 to 9.0 ppm) and between physisorbed water and iOH (1.1 – 4.0 ppm), indicating that all silanol groups are associated with physisorbed water, either through chemical exchange or spatial proximity.

The two-dimensional NOESY spectrum of epoxy-silica (Fig. 1b) is well resolved and shows diagonal peaks from the epoxy-linker (0 – 3.5 ppm), physisorbed water (4.0 ppm, a shoulder on the intense peak at 3.25 ppm from the epoxy-linker), and hBS groups (4.5 – 10.0 ppm). The spectrum also reveals cross peaks between protons in the epoxy-linker (with the green labels); these cross peaks may be ascribed to spin diffusion as the linker protons are non-exchangeable. Cross peaks are also observed between hBS and the 1, 2, 3, 4, 5 and $SiOCH_3$ protons in the epoxy-linker. This is probably a consequence of the relatively long mixing time (100 ms) used, with spin diffusion producing long-range magnetization transfer. It is worth noting the weak cross peak (highlighted in yellow, but below the plotted contour levels on the other side of the diagonal in Fig. 1b) between proton 6 from the epoxy-ring (2.4 ppm) and the hBS groups (5.5 ppm), highlighted in yellow. This indicates that some of the epoxy groups have opened to form diols and that the hydroxyl protons are either in close proximity or chemical exchange with hBS groups on the surface of silica. Finally, partly resolved cross peaks (0.8 – 4.0 ppm), (1.4 – 4.0 ppm), (3.0 – 4.0 ppm) can be observed in Fig. 1b between the 1, 2, 3, 4, 5 and $SiOCH_3$ protons in the epoxy-linker with the physisorbed water (highlighted in red). It is worth noting the 0.8 ppm shift of the 1 protons in the cross peak with the water, rather than the 0.4 ppm seen elsewhere, indicating a possible specific interaction with the physisorbed water. However, no noticeable changes in chemical shifts could be observed for the 2, 3, 4, 5 and $SiOCH_3$ protons in the epoxy-linker. Note that, although synthesis of epoxy-silica was performed under non-aqueous conditions, the peak at 4.0 ppm can be ascribed to water physisorbed from the atmosphere due to the hygroscopic nature of silica.

The ^{1}H NOESY spectra of [U-^{15}N]/hCA II (Fig. 1c) and [^{15}N Leu]/hCA II (Fig. 1d) immobilized on epoxy-silica are very similar, as expected, and reveal diagonal peaks from the epoxy-linker (0 – 3.5 ppm), water (4.0, 5.0 ppm) and from the aromatic and amide protons in the immobilized enzyme (6 – 10 ppm), highlighted with green, blue and red labels respectively. It is worth noting the two distinct water peaks at 4 and 5 ppm. The partly resolved water peak at 4 ppm can be ascribed to water physisorbed onto the surface of the epoxy-silica, while the water peak at 5 ppm can be ascribed to water associated with the immobilized enzyme (protein-associated water is usually observed at ~4.7 ppm).[40] These spectra also reveal cross peaks between protons from the epoxy-linker (0 – 4 ppm), epoxy-linker and water (0 to 4 ppm – 5 ppm), epoxy-linker and hCA II (0 to 4 ppm – 6 to 10 ppm), and also between water and hCA II (5 – 6 to 10 ppm).

To ascertain spatial proximities utilizing the ^{1}H-^{1}H dipolar coupling in a coherent process, two-dimensional ^{1}H double–single quantum (DQ-SQ) experiments using BABA recoupling were performed. The DQ-SQ NMR experiments selectively excite pairs of ^{1}H nuclei that are strongly dipolar coupled and, as a result, mobile or isolated protons are normally not observed. Figure 3 shows the ^{1}H DQ-SQ NMR spectra of (a) epoxy-silica, (b) [U-^{15}N]/hCA II immobilized on epoxy-silica and (c) [^{15}N Leu]/hCA II immobilized on epoxy-silica. These spectra were recorded at room temperature with one rotor period of recoupling on a B_0 = 20 T magnet at a MAS frequency of ν_R = 75 kHz. Our DQ-SQ experiments on silica were unsuccessful as the recoupling was inefficient owing to the mobility of the water molecules (data not shown).

The DQ-SQ spectrum of epoxy-silica (Fig. 3a) is well resolved and reveals pairs of correlated peaks, with the same F1 frequency and equidistant from the +2

diagonal, arising from protons that are close in space. The DQ-SQ correlation peaks from protons in the epoxy-linker are shown connected by dotted green lines, while the correlation peaks from protons in the epoxy-linker and the hBS groups are shown connected by dotted cyan lines. Well-resolved pairs of correlation peaks are observed for the 1 and 2 protons (F2: 0.4 –1.4 ppm), the 1 proton and $SiOCH_3$ (F2: 0.4 – 3.1 ppm) and the 2 and 3 protons (F2: 1.4 – 3.3 ppm) corresponding to their close proximities in space. The unsymmetrical peaks appearing around 3 ppm in F2 probably arise as a result of t_1 noise from the adsorbed water.

The DQ-SQ spectra of [U-^{15}N]/hCA II immobilized on epoxy-silica (Fig. 3b) and [^{15}N Leu]/hCA II immobilized on epoxy-silica (Fig. 3c) are very similar and consist of pairs of correlation peaks from the epoxy-linker, protons 1 and 2 (F2: 0.4 – 1.4 ppm), 2 and 3 (F2: 1.4 – 3.3 ppm), plus a range of correlation peaks connecting protons 3, 4 and 5 and the immobilized hCA II (a few pairs are highlighted with dotted red lines). Interestingly, we do not observe any correlation peaks connecting 1 and H2 protons in the epoxy-linker with protons in the immobilized hCA II, indicating that these protons are not close in space. These 1 and 2 protons in the epoxy linker are expected to be found close to the silica surface and the absence of any correlation peaks with the hCA II may indicate that immobilized enzyme is not in close contact with the silica surface. Thus the epoxy-linker may be acting as a cushion between the silica surface and the protein, thereby preventing any strong charge interactions that might lead to protein denaturation. Similar studies involving reconstitution of transmembrane proteins anchored into polymer-supported cushioned lipid bilayers have shown increased incorporation and enhanced enzymatic activity when compared with the reconstituted enzyme.[41]

Finally, in order to help understand the state of the enzyme after immobilization, a ^{1}H-detected MAS NMR (^{1}H-^{15}N) correlation experiment was performed at B_0 = 20 T and a MAS frequency of ν_R = 75 kHz. Figure 4 compares the resulting spectrum of [U-^{15}N]/hCA II in the immobilized state (Fig. 4b) with the solution-state TROSY-HSQC (Transverse Relaxation-Optimized Spectroscopy – Heteronuclear Single Quantum Coherence)[42] NMR spectrum of hCA II (Fig. 4a). Comparison of the two spectra reveals that majority of the peaks in the central region are well preserved, while the overall distribution of the peaks from the immobilized hCA II indicates that the structural integrity of the enzyme is well preserved on immobilization. Additional high frequency peaks (> 11 ppm in the ^{1}H dimension) in the immobilized state can be ascribed to strong hydrogen bonds in the solid that are broken upon dissolution.

Overall, a smaller number of resonances are observed from the hCA II in the immobilized state (Fig. 4b) compared with the solution-state HSQC NMR spectrum (Fig. 4a). The solution-state HSQC NMR experiment is based on INEPT-type (Insensitive Nuclei Enhanced by Polarization Transfer)[43] coherence transfer through *J* couplings, which works efficiently for many liquid samples. In solid-state NMR, INEPT signals from proteins are normally observed from residues that have sufficient mobility to average out anisotropic interactions and yield narrow resonances. We did not observe any signals from immobilized hCA II using INEPT-based experiments (data not shown). In contrast, ^{1}H-detected MAS NMR experiments rely on the method of cross polarization (CP) via heteronuclear through-space dipolar couplings,[33-35] which works efficiently for rigid solid samples. It seems likely that the absence of many of the cross peaks in Fig. 4b can be attributed to static disorder within the sample leading to enhanced line broadening, as has been reported

previously in the case of proteins entrapped in bioinspired silica.[23] It should be noted that, although we are suggesting that the structural integrity of the enzyme is well preserved on immobilization, this does not mean that the sample is not highly disordered. In addition to some likely disorder of the tertiary structure, individual protein molecules can be expected to be tethered to the silica surface by a variable number of linker molecules and to have a very wide range of orientations with respect to the surface, which itself will be highly heterogeneous. ^{1}H-detected experiments on [^{15}N Leu]/hCA II immobilized on epoxy-silica were not successful (data not shown) owing to the very much smaller number of expected resonances (26 Leu residues) consequent upon selective ^{15}N isotopic labelling and to the limited experimental sensitivity arising from the smaller amount of protein grafted onto the surface of the epoxy-silica support (9.9 mg of protein per 100 mg of support).[27]

Conclusions

In conclusion, we have demonstrated that ^{1}H and ^{1}H-detected solid-state NMR experiments performed at high magnetic fields and utilizing fast MAS can be successful in gaining insight into ^{1}H environments in silica, epoxy-silica and enzymes covalently immobilized on epoxy-silica. Most importantly, our results confirm our earlier result that the structural integrity of the protein is not drastically changed, but is well preserved upon covalent immobilization.[27] This had added significance when related to our previous observation that this immobilized enzymatic system retains 71% of its effective specific activity when compared with free hCA II in solution.[27] We believe that the outcomes of this present work are not limited to the better understanding of heterogeneous biocatalysts, but also to wider areas of

biotechnological processes and applications involving interactions of proteins with solid surfaces and supports.

Conflicts of interest

There are no conflicts to declare.

Acknowledgements

We thank the Leverhulme Trust (award RPG-2013-361) for financial support. We are indebted to Dr Kaspar Zimmermann for preparation of all protein constructs, Dr Elisa Nogueira for assistance, and the Swiss National Science Foundation for a grant to DH (SNF 200021_130263). The UK 850 MHz Solid-State NMR Facility used in this research was funded by EPSRC and BBSRC (contract reference PR140003), as well as the University of Warwick including via partial funding through Birmingham Science City Advanced Materials Projects 1 and 2 supported by Advantage West Midlands (AWM) and the European Regional Development Fund (ERDF). Collaborative assistance from the 850 MHz Facility Manager (Dr. Dinu Iuga, University of Warwick) is gratefully acknowledged. We also thank Daiso Chemical Co. Ltd, Japan, for donating the silica support used in this research.

References

1. F. Rusmini, Z. Zhong and J. Feijen, *Biomacromolecules*, 2007, **8**, 1775-1789.
2. A. Kuchler, M. Yoshimoto, S. Luginbuhl, F. Mavelli and P. Walde, *Nat. Nanotechnol.*, 2016, **11**, 409-420.
3. D. N. Tran and K. J. Balkus, *ACS Catal.*, 2011, **1**, 956-968.
4. R. A. Sheldon and S. van Pelt, *Chem. Soc. Rev.*, 2013, **42**, 6223-6235.

5. R. DiCosimo, J. McAuliffe, A. J. Poulose and G. Bohlmann, *Chem. Soc. Rev.*, 2013, **42**, 6437-6474.

6. P. V. Bower, E. A. Louie, J. R. Long, P. S. Stayton and G. P. Drobny, *Langmuir*, 2005, **21**, 3002-3007.

7. P. Xue, F. Xu and L. Xu, *Appl. Surf. Sci.*, 2008, **255**, 1625-1630.

8. M. Park, S. S. Park, M. Selvaraj, D. Zhao and C.-S. Ha, *Microporous Mesoporous Mater.*, 2009, **124**, 76-83.

9. S. B. Hartono, S. Z. Qiao, J. Liu, K. Jack, B. P. Ladewig, Z. Hao and G. Q. M. Lu, *J. Phys. Chem. C*, 2010, **114**, 8353-8362.

10. T. Weidner, N. F. Breen, K. Li, G. P. Drobny and D. G. Castner, *Proc. Natl. Acad. Sci. U.S.A.*, 2010, **107**, 13288-13293.

11. N. E. Fauré, P. J. Halling and S. Wimperis, *J. Phys. Chem. C*, 2014, **118**, 1042-1048.

12. Z. Zhou, F. Piepenbreier, V. R. R. Marthala, K. Karbacher and M. Hartmann, *Catal. Today*, 2015, **243**, 173-183.

13. C. Guo and G. P. Holland, *J. Phys. Chem. C*, 2015, **119**, 25663-25672.

14. J. M. Bolivar, I. Eisl and B. Nidetzky, *Catal. Today*, 2016, **259**, Part 1, 66-80.

15. L. Cerofolini, S. Giuntini, A. Louka, E. Ravera, M. Fragai and C. Luchinat, *J. Phys. Chem. B*, 2017, **121**, 8094-8101.

16. G. Goobes, P. S. Stayton and G. P. Drobny, *Prog. Nucl. Magn. Reson. Spectrosc.*, 2007, **50**, 71-85.

17. W. Y. Chow, R. Rajan, K. H. Muller, D. G. Reid, J. N. Skepper, W. C. Wong, R. A. Brooks, M. Green, D. Bihan, R. W. Farndale, D. A. Slatter, C. M. Shanahan and M. J. Duer, *Science*, 2014, **344**, 742-746.

18. W. J. Shaw, *Solid State Nucl. Magn. Reson.*, 2015, **70**, 1-14.

19. M. J. Duer, *J. Magn. Reson.*, 2015, **253**, 98-110.

20. K. H. Mroue, Y. Nishiyama, M. K. Pandey, B. Gong, E. McNerny, D. H. Kohn, M. D. Morris and A. Ramamoorthy, *Sci. Rep.* 2015, **5**, 11991.

21. E. Ravera, V. K. Michaelis, T.-C. Ong, E. G. Keeler, T. Martelli, M. Fragai, R. G. Griffin and C. Luchinat, *ChemPhysChem*, 2015, **16**, 2751-2754.

22. T. Martelli, E. Ravera, A. Louka, L. Cerofolini, M. Hafner, M. Fragai, C. F. W. Becker and C. Luchinat, *Chem. Eur. J.*, 2016, **22**, 425-432.

23. E. Ravera, L. Cerofolini, T. Martelli, A. Louka, M. Fragai and C. Luchinat, *Sci. Rep.*, 2016, **6**, 27851.

24. E. Ravera, T. Martelli, Y. Geiger, M. Fragai, G. Goobes and C. Luchinat, *Coord. Chem. Rev.*, 2016, **327**, 110-122.

25. S. I. Brückner, S. Donets, A. Dianat, M. Bobeth, R. Gutiérrez, G. Cuniberti and E. Brunner, *Langmuir*, 2016, **32**, 11698-11705.

26. X. Yang, F. Huang, X. Xu, Y. Liu, C. Ding, K. Wang, A. Guo, W. Li and J. Li, *Chem. Mater.*, 2017, **29**, 5663-5670.

27. S. Varghese, P. J. Halling, D. Häussinger and S. Wimperis, *J. Phys. Chem. C*, 2016, **120**, 28717-28726.

28. R. Zhang, K. H. Mroue and A. Ramamoorthy, *Acc. Chem. Res.*, 2017, **50**, 1105-1113.

29. S. K. Nair, T. L. Calderone, D. W. Christianson and C. A. Fierke, *J. Biol. Chem.*, 1991, **266**, 17320-17325.

30. L. Zheng, U. Baumann and J.-L. Reymond, *Nucleic Acids Res.*, 2004, **32**, e115.

31. J. Jeener, B. H. Meier, P. Bachmann, and R. R. Ernst, *J. Chem. Phys.*, 1979, **71**, 4546-4553.

32. W. Sommer, J. Gottwald, D. E. Demco and H. W. Spiess, *J. Magn. Reson., Ser. A*, 1995, **113**, 131-134.

33. A. Pines, M. G. Gibby and J. S. Waugh, *J. Chem. Phys.*, 1973, **59**, 569-590.

34. J. Schaefer and E. O. Stejskal, *J. Am. Chem. Soc.*, 1976, **98**, 1031-1032.

35. G. Metz, X. L. Wu and S. O. Smith, *J. Magn. Reson.*, 1994, **110**, 219-227.

36. B. M. Fung, A. K. Khitrin and K. Ermolaev, *J. Magn. Reson.*, 2000, **142**, 97-101.

37. M. K. Pandey, S. Vivekanandan, K. Yamamoto, S. Im, L. Waskell and A. Ramamoorthy, *J. Magn. Reson.*, 2014, **242**, 169-179.

38. B. Grünberg, T. Emmler, E. Gedat, I. Shenderovich, G. H. Findenegg, H.-H. Limbach and G. Buntkowsky, *Chem. Eur. J*, 2004, **10**, 5689-5696.

39. G. E. Maciel, *J. Am. Chem. Soc.*, 1996, **118**, 401-406.

40. A. Lesage and A. Böckmann, *J. Am. Chem. Soc.*, 2003, **125**, 13336-13337.

41. L. Renner, T. Pompe, R. Lemaitre, D. Drechsel and C. Werner, *Soft Matter*, 2010, **6**, 5382-5389.

42. K. Pervushin, R. Riek, G. Wider and K. Wüthrich, *Proc. Natl. Acad. Sci. U.S.A.*, 1997, **94**, 12366-12371.

43. G. A. Morris and R. Freeman, *J. Am. Chem. Soc.*, 1979, **101**, 760-762.

Figure Legends

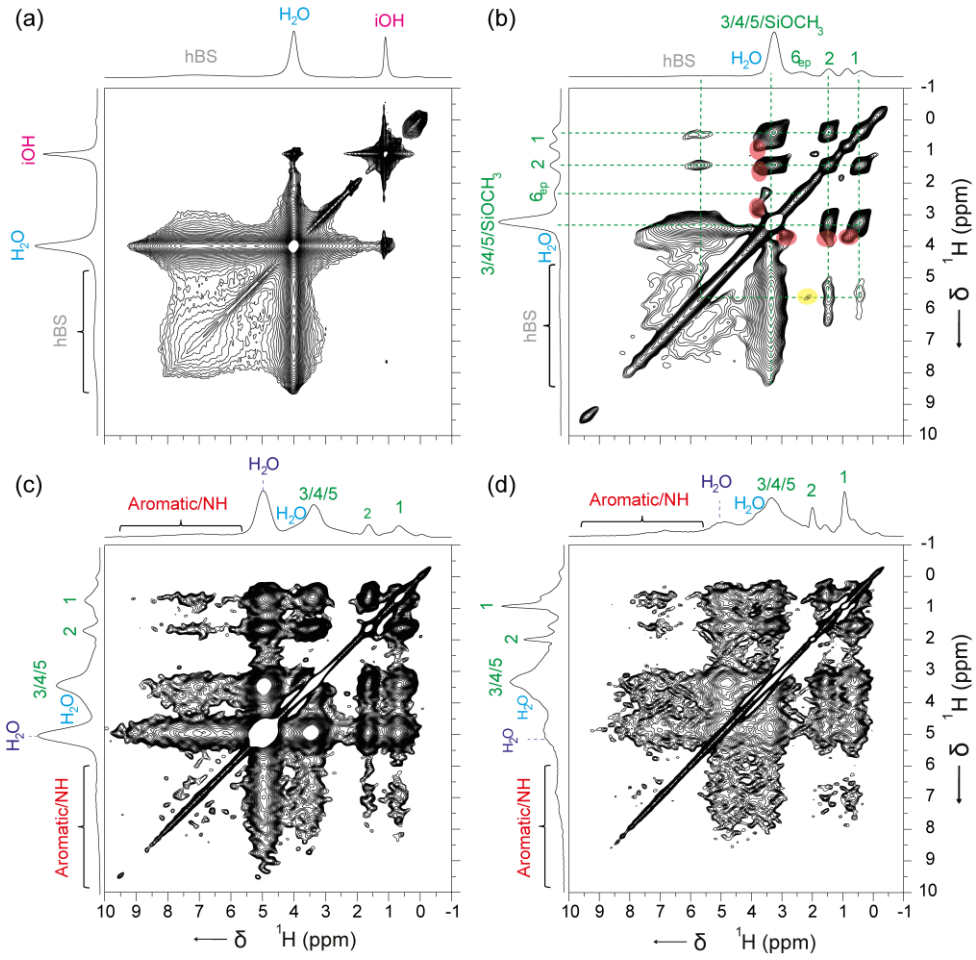

Fig. 1. Two-dimensional ^{1}H-^{1}H NOESY-type spectra of (a) silica, (b) epoxy-silica, (c) [U-^{15}N]/hCA II immobilized on epoxy-silica and (d) [^{15}N Leu]/hCA II immobilized on epoxy-silica. Spectra were recorded using 100 ms mixing time at B_0 = 20 T and a MAS frequency of ν_R = 75 kHz. Spectra were acquired using 8 transients for each of 300 t_1 increments of 53.3 μs using a recycle interval of 2 s. Spectrum (a) was processed with 50 Hz line broadening in both F1 and F2 dimensions; the remainder were processed using a resolution enhancement function (Bruker parameters LB = –150 Hz and GB = 0.2) in both F1 and F2 dimensions. The chemical shift assignments

use the scheme shown in Fig. 2. The cross peaks highlighted in red and yellow are discussed in the text.

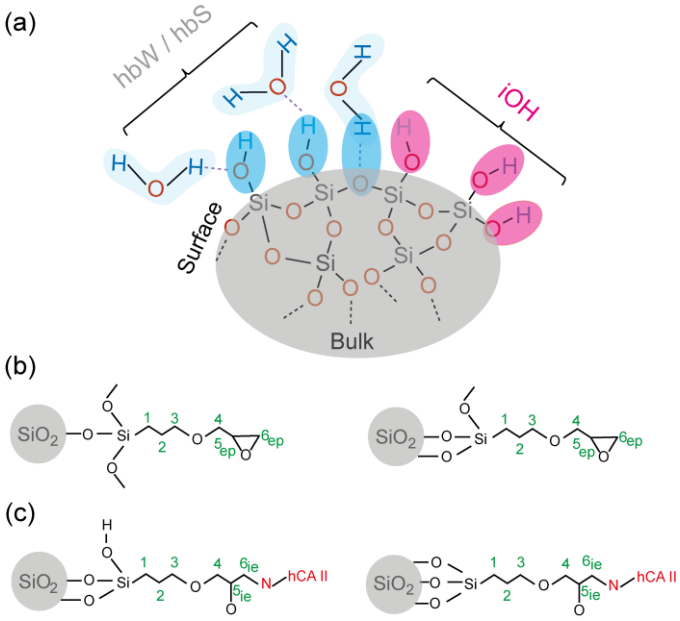

Fig. 2. Simplified schematic representation of (a) bare silica, (b) epoxy-silica before immobilization and (c) epoxy-silica after immobilization with hCA II. Two possible modes of connection of the linker to the silica surface are shown in (b) and (c).

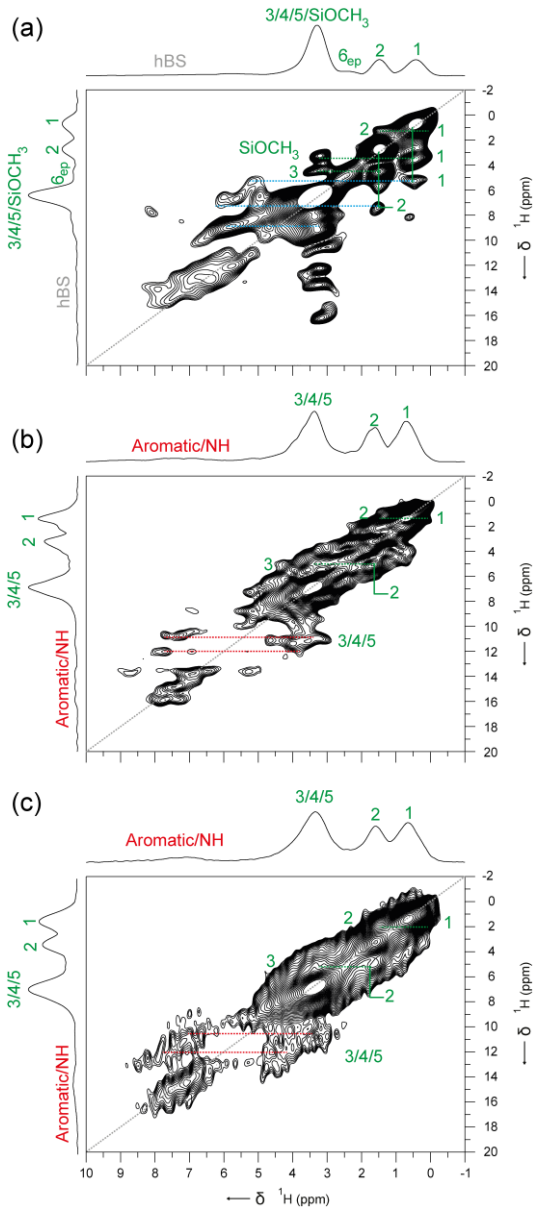

Fig. 3. Two-dimensional ^{1}H DQ-SQ spectra of (a) epoxy-silica, (b) [U-^{15}N]/hCA II immobilized on epoxy-silica and (c) [^{15}N Leu]/hCA II immobilized on epoxy-silica recorded at B_0 = 20 T and a MAS rate of ν_R = 75 kHz. Spectra were acquired using 16 transients for each of the 128 t_1 increments of 13.3 μs using a recycle interval of 2 s. Spectra were processed using a resolution enhancement function (Bruker parameters LB = –150 Hz and GB = 0.2) in both F1 and F2 dimensions. The chemical shift assignments use the scheme shown in Fig. 2.

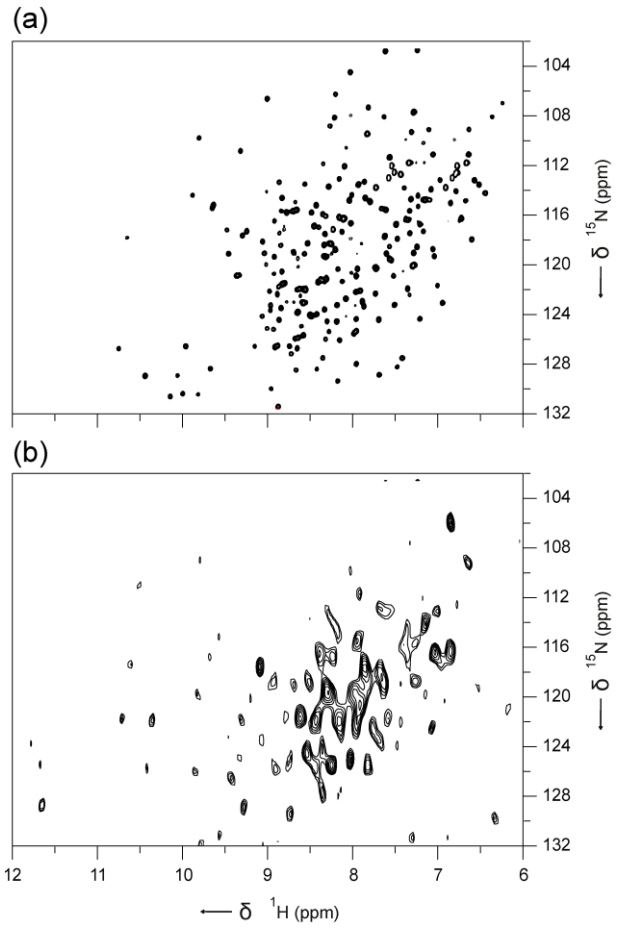

Fig. 4. (a) Solution-state TROSY[36]-HSQC NMR spectrum of hCA II and (b) ^{1}H-detected (^{1}H-^{15}N) MAS NMR spectrum of [U-^{15}N]/hCA II in the immobilized state. The solution-state NMR spectrum of [U-^{15}N]/hCA II was acquired at B_0 = 14.1 T using 64 transients for each of the 256 t_1 increments of 500 µs using a recycle interval of 1 s magnet. The spectrum of the [U-^{15}N]/hCA II in the immobilized state was acquired at B_0 = 20 T and a MAS frequency of ν_R = 75 kHz using 1024 transients for each of the 40 t_1 increments of 290 µs using a recycle interval of 2 s. The spectra were processed without any window functions.